

Ferrimagnetic devitrified glass doped with copper by ion exchange: Microstructure, bioactivity and antibacterial properties

Original

Ferrimagnetic devitrified glass doped with copper by ion exchange: Microstructure, bioactivity and antibacterial properties / Miola, M.; Bruno, M.; Verne, Enrica.. - In: CERAMICS INTERNATIONAL. - ISSN 0272-8842. - 50:8(2024), pp. 12737-12745. [10.1016/j.ceramint.2024.01.178]

Availability:

This version is available at: 11583/2988865 since: 2024-05-20T14:48:21Z

Publisher:

Elsevier

Published

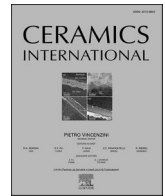
DOI:10.1016/j.ceramint.2024.01.178

Terms of use:

This article is made available under terms and conditions as specified in the corresponding bibliographic description in the repository

Publisher copyright

(Article begins on next page)



Ferrimagnetic devitrified glass doped with copper by ion exchange: Microstructure, bioactivity and antibacterial properties

Marta Miola^{*}, Matteo Bruno, Enrica Vernè

Politecnico di Torino, Applied Science and Technology Department, Corso Duca degli Abruzzi 24, 10129, Torino, Italy

ARTICLE INFO

Handling Editor: Dr P. Vincenzini

Keywords:

Ferrimagnetic devitrified glass
Copper
Antibacterial
Bone tumor
Infection prevention

ABSTRACT

In this work, the ion-exchange technique in molten salts was investigated to introduce copper ions in a bioactive and ferrimagnetic devitrified glass. This approach aimed to develop a magnetic and bioactive material for oncologic bone implants, able to join the ability to promote bone bonding to hyperthermic therapy while simultaneously lowering the risk of developing post-surgery infections. The ion-exchange approach was developed in order to overcome experimental critical issues related to the influence of copper introduction as a starting reagent, during the material synthesis, on magnetite nucleation.

The magnetic devitrified glass was prepared by melt and quenching route, followed by ion exchange in a mixture of molten sodium and copper nitrates, in three different Na/Cu molar ratios (20, 200, 2000). The obtained samples were analysed in terms of morphology, composition, ability to release heat, bioactivity and antibacterial properties. The results revealed that copper ion-exchange involved both sodium and calcium ions and the precipitation of few amounts of copper oxide aggregates occurred. The crystalline nature of the starting material and its ability to reach the temperature needed for hyperthermia, under exposition to an alternating magnetic field, were not affected. A bacteriostatic effect was obtained by samples with the highest copper amount and the copper doping did not affect the bioactivity of the glass ceramic.

1. Introduction

Bioactive glasses and glass-ceramics have been studied for decades for their ability to chemically bind to bone tissue and promote its regeneration [1–4]. The versatility of bioactive glasses has prompted researchers to modify the composition of these materials to improve their biological activity, by introducing therapeutic elements in their composition or inducing the formation of second phases [5–7]. In particular, the nucleation of magnetic phases inside a bioactive glass matrix gained great interest in producing glass-ceramic/devitrified materials for treating tumors through hyperthermia [7,8].

Despite the low incidence of malignant bone tumors, the degree of mortality connected to this pathology is extremely high [9]. Actually, bone tumors are surgically treated by performing a wide and invasive local excision or an amputation. Surgery is often combined with chemotherapy and radiotherapy, which remain the main therapies applied in the clinical setting. However, these treatments often imply side effects and are not completely determined. Alternative therapies, such as photodynamic therapy, hyperthermia, immunotherapy, gene

therapy, and hormone therapy have been proposed and are being studied. Among them, hyperthermia has been recognized as an effective treatment of solid tumors [10], and its effectiveness, when applied in combination with chemo and radiotherapy, has been widely demonstrated [11,12]. In particular, magnetic hyperthermia attracted the attention of researchers; magnetic materials (such as iron oxides, ferrites, metal alloys) can be implanted in the cavity originating from the removal of the tumor and release heat when subjected using an external alternating magnetic field [7,8,13,14] selectively killing tumor cells.

Magnetic hyperthermia has also several advantages: it can be repeated according to the patient's needs (for example in case of relapses, without resorting to invasive procedures; moreover, the therapy is targeted at the tumor site, it has no adverse effects on healthy tissues and can be used for both superficial and deep tumors [15].

For bone tumor treatment, the research has as focused on the development of magnetic and bioactive material, in particular bioactive glasses/glass-ceramics, to join the hyperthermic therapy and the ability to promote bone bonding (bioactivity) and to regenerate both hard and soft tissues, thanks to the release of therapeutic ions. In recent years,

^{*} Corresponding author. Politecnico di Torino Department of Applied Science and Technology (DISAT), Corso Duca degli Abruzzi 24, 10129, Torino, Italy.
E-mail address: marta.miola@polito.it (M. Miola).

<https://doi.org/10.1016/j.ceramint.2024.01.178>

Received 23 October 2023; Received in revised form 19 December 2023; Accepted 12 January 2024

Available online 14 January 2024

0272-8842/© 2024 The Authors. Published by Elsevier Ltd. This is an open access article under the CC BY license (<http://creativecommons.org/licenses/by/4.0/>).

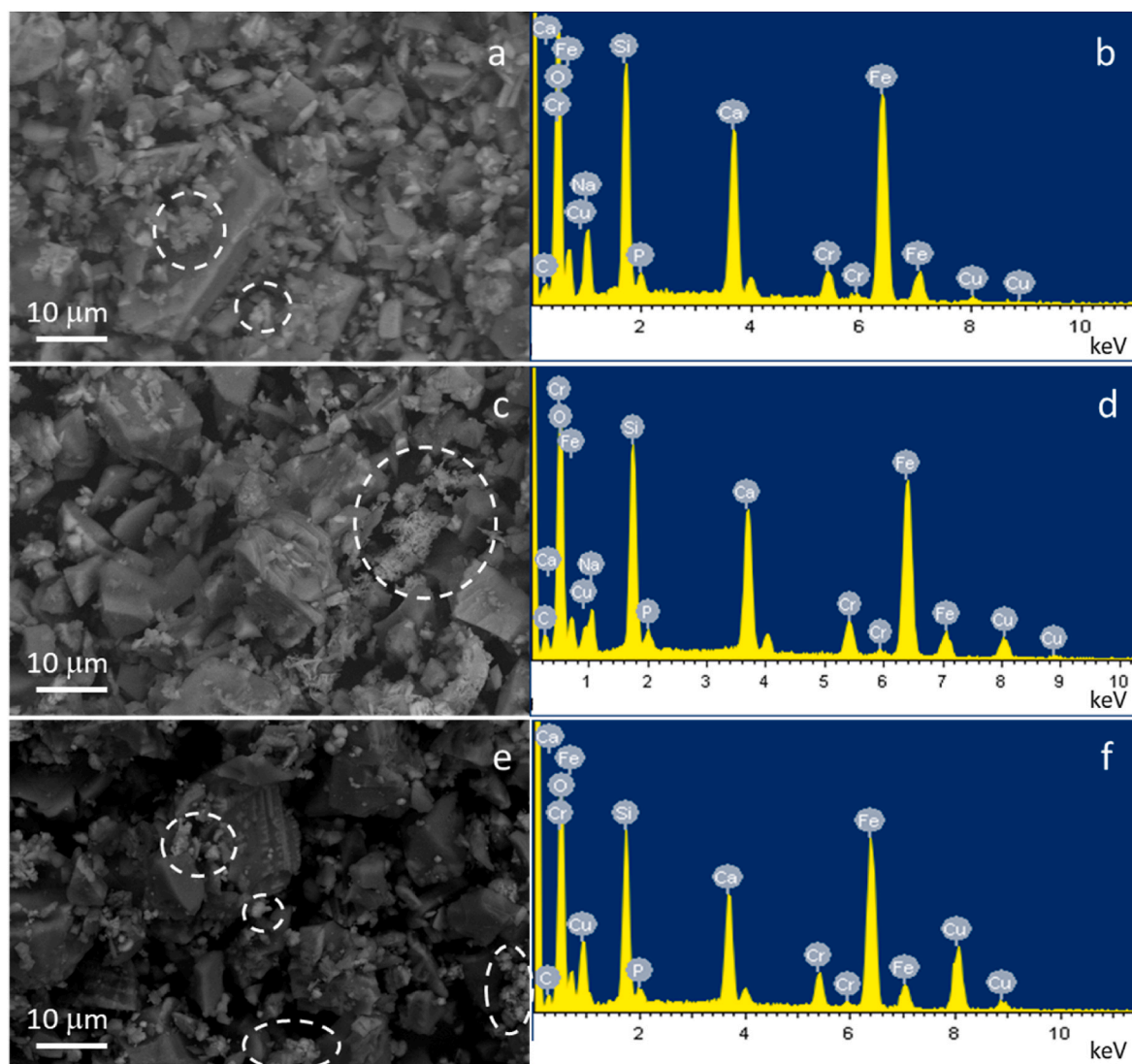


Fig. 1. FESEM-EDS analysis of SC45_Cu, using a $\text{NaNO}_3/\text{Cu}(\text{NO}_3)_2 \cdot 3\text{H}_2\text{O}$ molar ratio 2000 (a, b), 200 (c, d) and 20 (e, f).

various magnetic and bioactive glass/glass-ceramic compositions have therefore been proposed [7,8]. Magnetic and bioactive glasses/ceramics can be produced by means of melt and quenching technique [16–25] or via sol-gel [26–30], and the magnetic phase can be added to a bioactive composition or can nucleate during the material synthesis. Moreover, bioactive and magnetic glasses/glass-ceramics can be functionalized with antineoplastic drugs [31] to join chemotherapy and hyperthermia and can be used, in powder form, as fillers in polymethyl methacrylate (PMMA)-based cement [32–34].

Since one of the common issues connected to bone tumor surgery is the risk of developing infections, especially in patients already immunocompromised due to chemo and radiotherapies, magnetic and bioactive glasses/glass-ceramics have been also doped with antibacterial elements [35–37]. In particular, the authors investigated the magnetic and antibacterial properties of silver or copper doped ferrimagnetic and bioactive devitrified glass containing magnetite crystals (SC45), synthesized by melt and quenching process. The obtained results evidenced the ability to produce heat and good antibacterial properties for silver-doped samples; while the copper introduction as starting reagent during the material synthesis influenced the formation of magnetite and induced the nucleation of different crystalline phases, which in turn affected its ability to release heat. Moreover, the evaluation of antibacterial properties evidenced a limited copper

diffusion, useless to inhibit bacteria proliferation. However, different studies highlight important antimicrobial properties of copper and evidence that Cu shows no difference in sensitivity between Gram-positive and Gram-negative microorganisms [38,39].

For these reasons, in this work, the authors investigated a different approach to introduce copper ions in the 45S5 bioactive and ferrimagnetic composition. The ion-exchange technique in molten salts was explored, and the obtained samples were analysed in terms of morphology, composition, ability to release heat, bioactive and antibacterial properties.

2. Materials and method

2.1. Materials synthesis

The bioactive ferrimagnetic devitrified glass (SC45) with the following composition: 24.7 % SiO_2 -13.5 % CaO -13.5 % Na_2O -3.3 % P_2O_5 -31 % Fe_2O_3 -14 % FeO (wt%) was produced by melt and quenching technique. As previously reported [35], the reactants were mechanically mixed, placed in a Pt crucible and melted at 1550 °C (Nabertherm-Carbolite 1800) for 25 min, using a heating rate of 10 °C/min. The melt was poured into a brass mold and subsequently milled (using a tungsten carbide grinding jar) and sieved to obtain powders with

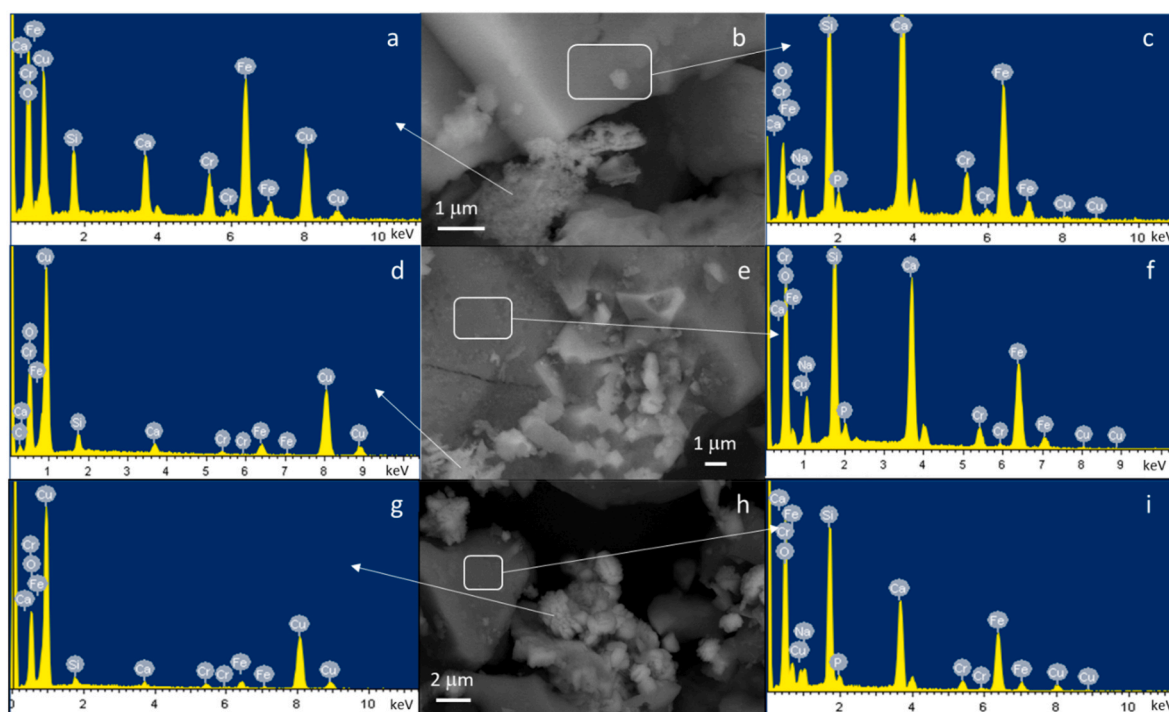


Fig. 2. FESEM-EDS analysis of SC45_Cu, using a $\text{NaNO}_3/\text{Cu}(\text{NO}_3)_2 \cdot 3\text{H}_2\text{O}$ molar ratio 2000 (a-c), 200 (d-f) and 20 (g-i).

particle sizes below 20 μm . In order to introduce copper in the SC45 composition, the ion exchange technique in molten salts has been used. The ion exchange process was carried out with a silica crucible, 1 g of SC45 and 20 g of mixture of sodium nitrate (NaNO_3) and copper nitrate ($\text{Cu}(\text{NO}_3)_2 \cdot 3\text{H}_2\text{O}$), in three different Na/Cu molar ratios (20, 200, 2000). The ion exchange in molten salt was performed at 380 $^\circ\text{C}$ for 30 min with a heating rate of 10 $^\circ\text{C}/\text{min}$, then powders were cooled at room temperature and washed with bi-distilled water in ultrasounds two times. Finally, the copper-doped powders (SC45_Cu) were filtered and dried in an oven at 60 $^\circ\text{C}$ overnight. All reagents for materials preparation were purchased by Sigma Aldrich.

2.2. Materials characterization

The morphology and composition of SC45_Cu were investigated by means of field emission electron microscopy (FESEM – SUPRATM 40, Zeiss) equipped with energy dispersion spectrometry (EDAX PV 9900) after chromium-coating of the samples.

The effect of copper doping in the structure of the 45S5 was investigated by X-Ray diffraction (X'Pert Philips diffractometer), using the Bragg Brentano camera geometry with $\text{Cu-K}\alpha$ incident radiation, source voltage and current set at 40 kV and 30 mA, step size $\Delta(2\theta) = 0.02^\circ$, fixed counting time of 1 s per step. The acquired spectra were analysed using the “X'Pert High Score” program, with the PCPDFWIN database (2002 JCPDS- International Centre for Diffraction Data).

The heat generation of materials under exposition to an alternating magnetic field was evaluated by means of a magnetic induction furnace (Egma 6 - Felmi S.r.l) using a 220 kHz working frequency and 22.6 mT magnetic field. The measurements were performed on 0.5 g of devitrified glass powders placed in a glass tube containing 16 ml of distilled water, covered with a polyethylene foam thermal insulator to reduce the heat dispersion. The test was performed in triplicate and the temperature increase was measured after 2, 4, 6 and 8 min of treatment using a digital thermocouple.

The bioactivity of the samples doped with copper was investigated by immersion in simulated body fluid (SBF) for up to 4 weeks, employing morphological analysis, in order to detect eventual calcium

phosphate precipitates on their surface, and EDS analysis, for the evaluation of the compositional modification on the sample surface during soaking time. The pH of the solution was monitored during the whole test.

The antibacterial properties were investigated on copper-doped SC45 pellets through the inhibition halo test, in accordance with the National Committee for Clinical Laboratory Standard [40], using a standard strain of *Staphylococcus aureus* (ATCC 29213). The pellets were prepared by pressing 200 mg of powders at 4 tons for 10 s in an automatic press (Graseby-Specac T-40). The inhibition halo test was performed by preparing a 0.5 McFarland solution (Phoenix Spec BD McFarland), containing approximately $1 \cdot 10^8$ colony forming units (CFU)/ml, as described in Ref. [41]. The 0.5 McFarland suspension was homogeneously spread on Mueller Hinton agar plate; the samples were placed in contact with the agar and incubated overnight at 35 $^\circ\text{C}$. Subsequently, the inhibition zone was observed and measured.

3. Results and discussion

3.1. Morphology and composition

Fig. 1 reports the FESEM-EDS analysis of SC45_Cu using different ion-exchange conditions. The EDS spectra demonstrated an increasing copper amount with the decrease of $\text{NaNO}_3/\text{Cu}(\text{NO}_3)_2 \cdot 3\text{H}_2\text{O}$ molar ratio: SC45_Cu2000 showed a Cu at% of 2 ± 0.3 , SC45_Cu200 of 5.1 ± 0.3 and SC45_Cu20 of 59.9 ± 4 . The increase in Cu amount is accompanied by a strong decrease in Na and a slight decrease in Ca, suggesting that the ion-exchange process involved probably both Na^+ and Ca^{2+} ions, as already highlighted in other studies, in particular with high copper concentrations [41–43]. FESEM micrographs of samples after ion exchange evidenced the formation of small aggregates with morphology different from the devitrified glass particles (evidenced by circles).

Fig. 2 shows the FESEM-EDS analysis at a higher magnification of SC45_Cu samples. In all samples, small aggregates rich in copper are detectable, most likely generated during the ion exchange process, as previously observed by the authors with other glass compositions [43]. The EDS analysis in areas without precipitates evidenced small amounts

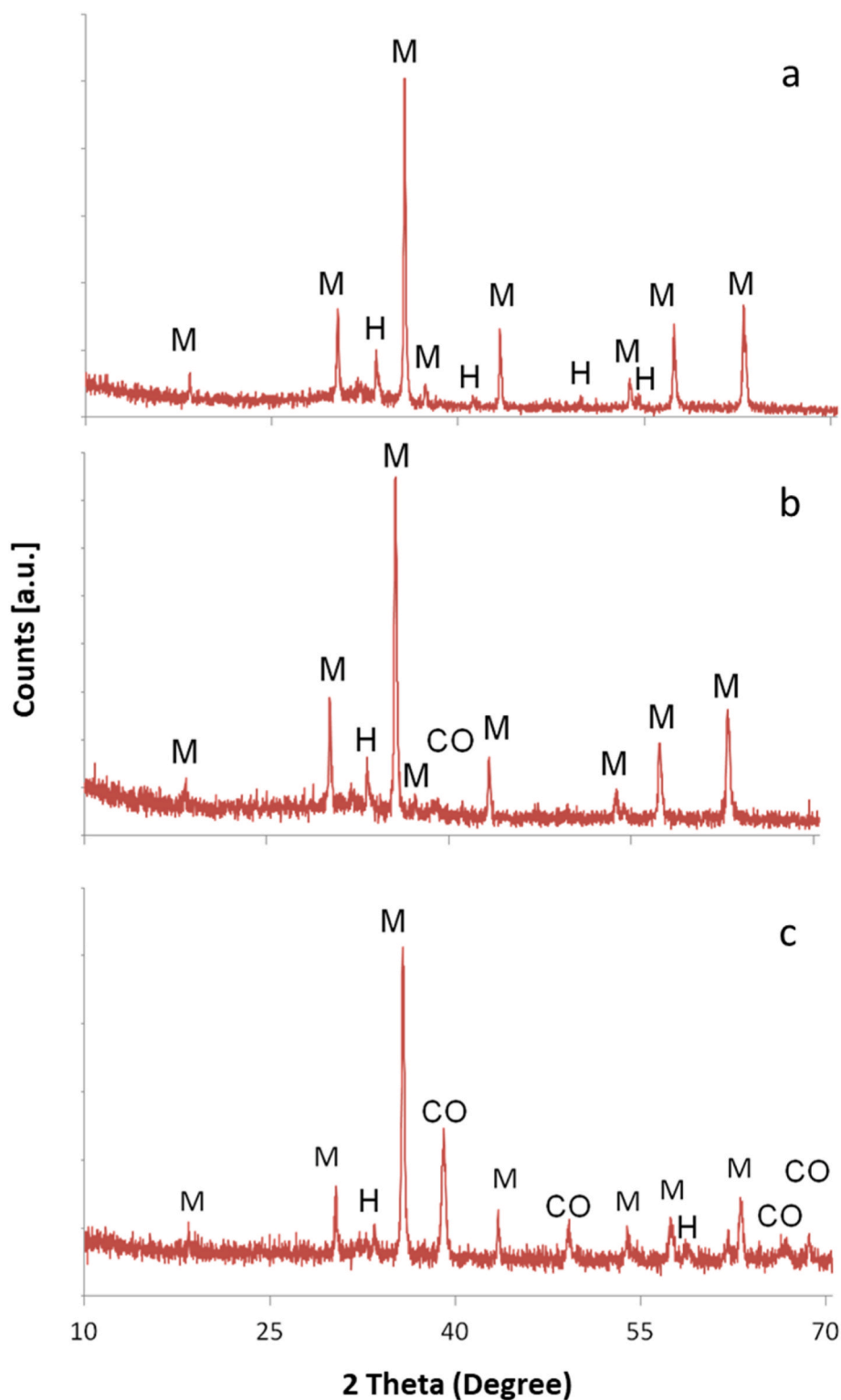


Fig. 3. XRD spectra of SC45_Cu2000 (a), SC45_Cu200 (b) and SC45_Cu20 (c). M = magnetite, H = hematite, CO = copper oxide.

of Cu in the SC45 particles (Fig. 2c–f and i). The presence of copper in ionic form, which can be easily released from the material, is useful for imparting important antibacterial properties. As already reported by other authors [44,45], the bactericidal activity of copper is mainly ascribed to the release of copper ions, which damage the bacterial cell membrane and produce oxidative stress, resulting in the microorganisms' death.

3.2. Phase analysis

The XRD analysis of SC45_Cu is reported in Fig. 3. As it can be observed, in addition to magnetite, a small amount of hematite and copper oxide, in greater amount as the concentration of copper in the ion-exchange conditions is increased, can be detected. Mainly for SC45_Cu20 (Fig. 3c), well-defined copper oxide (CuO) peaks can be detected at about 2 theta = 35 (covered by magnetite peak), 39, 48, 66,

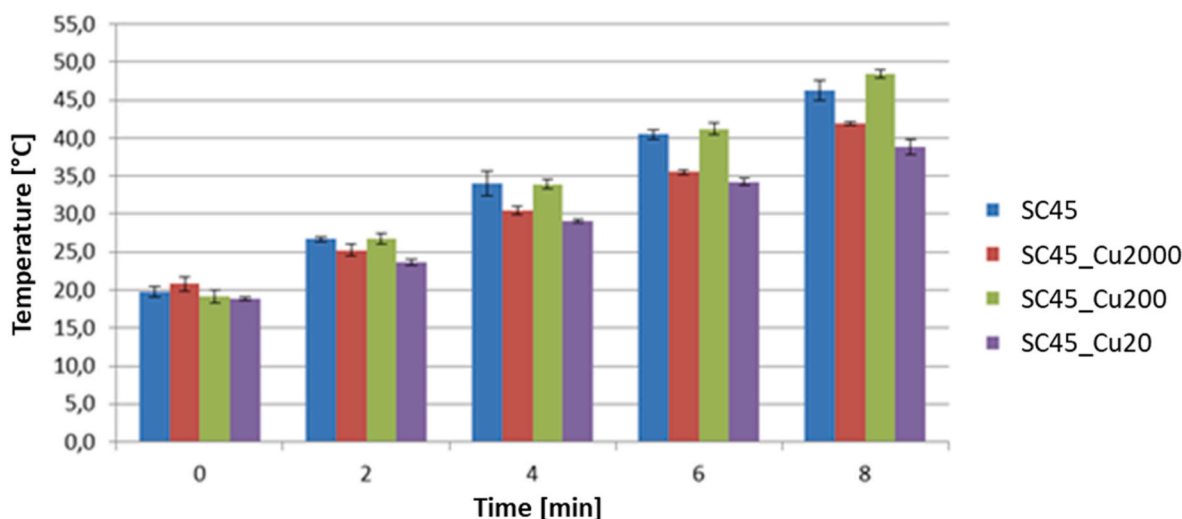


Fig. 4. Temperature increment registered during the calorimetric test on SC45, SC45_Cu2000, SC45_Cu200 and SC45_Cu20.

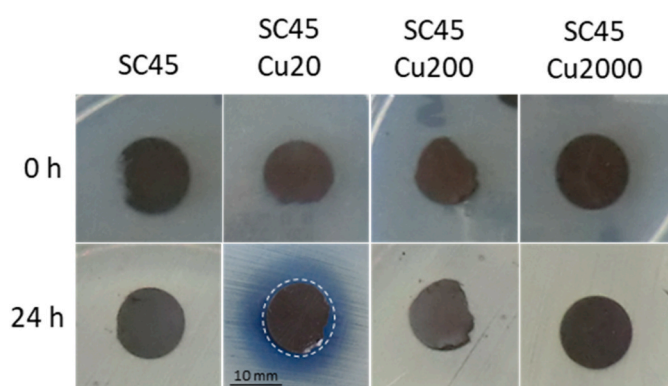


Fig. 5. images of SC45, SC45_Cu2000, SC45_Cu200 and SC45_Cu20 samples on Mueller Hinton agar plate after the incubation at 35 °C for 24 h.

68 (reference code 01-089-5898), together with magnetite (ref. code 01-089-3854) and a small amount of hematite (ref. code 01-073-0603). These results are in agreement with the FESEM observations, supporting the hypothesis that, during the ion-exchange process, the precipitation of copper oxide aggregates occurred beyond the exchange of copper with sodium and calcium ions, particularly as the Cu concentration increases.

3.3. Calorimetric characterization

Fig. 4 reports the results of the calorimetric measurements on SC45_Cu samples.

The temperature increments of the copper-doped SC45 were slightly lower than the pure SC45, except for the SC45_Cu200 samples that exceeded 4.7 % SC45 at 8 min. However, at times lower than 8 min, SC45_Cu200 has the same heating behavior as SC45. Nevertheless, the differences among the samples do not appear to be of concern; considering the obtained delta and the body temperature (about 37 °C), all samples are able to reach in few minutes the temperature useful for hyperthermia (42–43 °C). Moreover, the obtained results evidenced that the ion-exchange process allowed to introduce copper in the devitrified glass composition, without affecting its ability to release heat, as instead observed by introducing copper as a starting reagent in the melt and quenching technique [36].

3.4. Antibacterial properties

The results of the antibacterial test (samples on Mueller Hinton agar plate after the incubation at 35 °C for 24 h) are shown in Fig. 5. Only the sample SC45_Cu20 reveals a small inhibition halo of about 1 mm (evidenced by a circle in Fig. 5), which is correlated to a bacteriostatic effect [40] and a blue diffusion halo, most likely owing to the release of free Cu^{++} ions from the amorphous network [46]. On the other hand, no inhibition nor diffusion halo was noticed for SC45_Cu200 and SC45_Cu2000 samples. As evidenced by the FESEM-EDS analyses, SC45_Cu2000 and Cu200 contain a low amount of Cu; moreover, as observed in Fig. 2 c,f,i, all samples contain CuO precipitates, which have demonstrated a poor antibacterial effect [46,47]. As highlighted by the authors in other works [36,41,46], the presence of Cu-containing crystalline phases or Cu in metallic form reduces the antibacterial effect of the materials, confirming once again that the bacteriostatic effect is mainly related to the presence of free copper ions in the residual glassy phase, able to be released and interact with the bacterial cell membrane. Despite the presence of CuO precipitates, the SC45_Cu20 sample still contains a substantial amount of Cu in ionic form (Cu^{++}), which diffuses in the agar and, as previously discussed [44,45], it is responsible for the formation of the inhibition halo and thus for the antibacterial action.

Therefore, this preliminary result is encouraging because it demonstrates that ion exchange is a useful technique to impart antibacterial properties to a ferrimagnetic devitrified glass, potentially beneficial for the treatment of tumor in hyperthermia, using Cu as antimicrobial agent. The ion exchange process, unlike the melt and quenching technique previously evaluated by the authors [36], limits the formation of crystalline phases and allows the introduction of a useful amount of copper ions, available to be released and to implement their antibacterial effect.

In a previous work [35], the authors evaluated the introduction of Ag in the same composition, assessing its antibacterial efficacy. The comparison between the effectiveness of different elements with antibacterial action is widely debated in the literature, with sometimes conflicting results; however, several studies report a higher antimicrobial efficacy of copper and no difference in sensitivity between Gram-positive and Gram-negative microorganisms, unlike what is observed for example for Ag and Zn [38,39].

3.5. Bioactivity

Fig. 6 a-d report the EDS surface analysis of copper-doped SC45

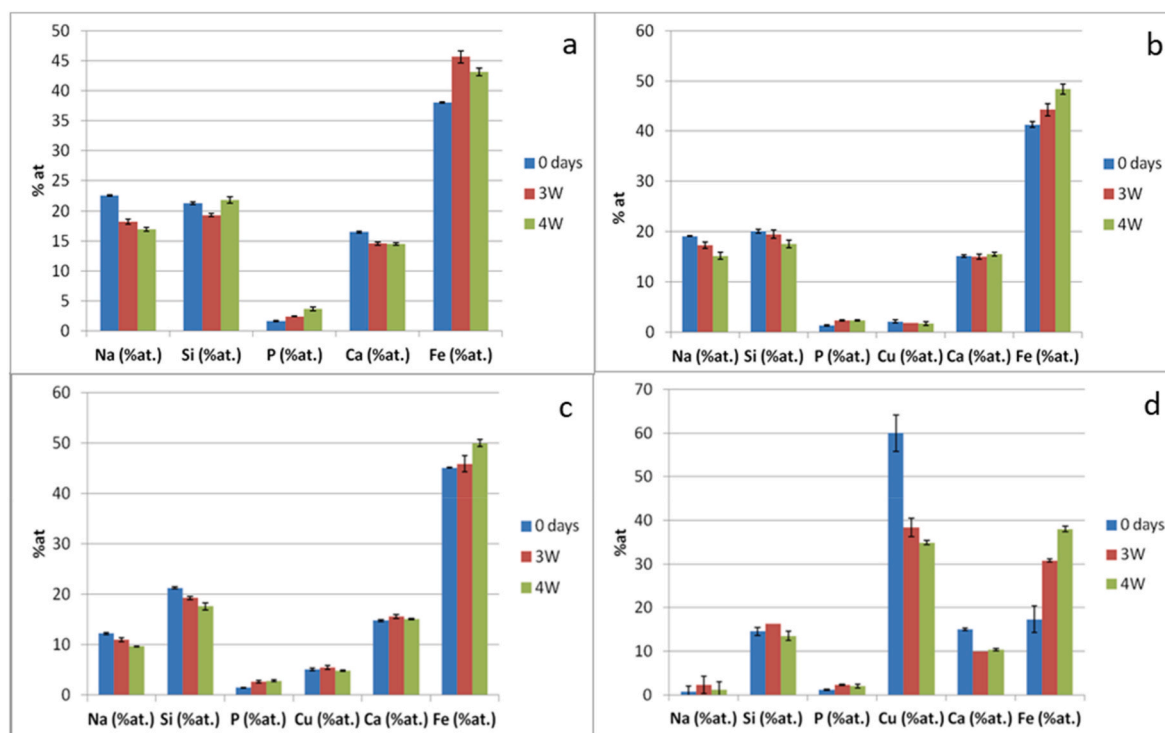


Fig. 6. Concentrations (at.%) of elements on the surface of SC45 (a) with respect to SC45_Cu2000 (b), SC45_Cu200 (c) and SC45_Cu20 (d) before and after in vitro bioactivity test.

compared to the control (SC45) at 0, 3 and 4 weeks in SBF. The reported values are a mean of three analyses performed on different surface points of each sample.

The trend is quite similar in all formulations: sodium (Na) concentration decreases at 3 and 4 weeks, which confirms the activation of the bioactivity mechanism. Silicon (Si) concentration decreases for SC45_Cu2000 and SC45_Cu200, while it remains almost stable for SC45_Cu20. Phosphorus (P) concentration increases for all formulations, probably due to the presence of a phosphate amorphous layer that can be identified as a precursor of hydroxyapatite. Calcium (Ca) concentration remains almost stable at each time point, revealing the slow reactivity of this material, already observed in previous works for undoped SC45 [48]. Iron (Fe) concentration increases gradually at 3 and 4 weeks for all devitrified glasses. The trend is influenced by the gradual dissolution of the amorphous matrix which allows the exposition of magnetite on the sample surface. Copper does not undergo significant variations in any sample, except for SC45_Cu20, where a sensible decrease is seen from 0 to three weeks, evidencing the release of copper ions, as also observed in the antibacterial test.

The trends of pH of the soaking solutions (data not reported) are quite similar for the various compositions and they oscillate in the physiological range between 7.4 and 7.8 at different time points. It can be assumed that the fluctuation is connected to the bioactivity of the amorphous phase of the material.

Fig. 7 reports a morphology and compositional analysis of copper-doped particles after 3 weeks in SBF, partially covered by some precipitates.

The morphological analysis of SC45_Cu20 after 3 weeks in SBF (Fig. 7a) shows the crystals of octahedral magnetite organized in a columnar shape embedded into the glass matrix. The EDS analysis displays high peaks of silicon, calcium and phosphorous, confirming the presence of calcium phosphate rich silica gel on the particle. Fig. 7b reports the morphology SC45_Cu200 after 3 weeks in SBF: the analysis shows a reaction layer that coated glass particle, ascribable to a calcium phosphate rich silica gel, as confirmed by the EDS analysis, that shows a

high peak of silicon, calcium and phosphorous. As previously observed for other samples, the surface of SC45_Cu2000 particles (Fig. 7c) shows some precipitates. The ratio comparison of the peaks of silicon, calcium and phosphorous detected in the local EDS, with respect to the same peaks of the EDS of area performed on the same sample before soaking in SBF (Fig. 1), evidences some differences probably due to the formation of a silica gel rich in calcium phosphates correlated to the intermediate steps of bioactivity [1,2] such as the precipitation of calcium phosphate precursors of HAp.

XRD investigation (not reported) did not detect any characteristic peaks of calcium phosphate crystalline phase, supporting the hypothesis that all the samples are characterized by a low bioactivity index.

Fig. 8 reports the morphology of copper-doped particles after 4 weeks in SBF, where some precipitates are evidenced. The local EDS of the particle shows a variation in silicon, phosphorous and calcium peaks ratio. Even in this case, we can assume that a calcium-rich silica gel precipitated on the particle without producing crystalline hydroxyapatite. In particular, the local EDS analysis of SC45_Cu2000 sample after 4 weeks in SBF (Fig. 8c) presents higher peaks of calcium and phosphorous.

However, also in this case, the XRD investigation on SC45_Cu2000, SC45_Cu200 and SC4_Cu20 after one month in SBF (data not reported) did not evidence any crystalline calcium phosphate phase.

In conclusion, the bioactivity investigation performed on SC45 doped with copper by ion exchange molten salt technique confirmed that the copper doping did not modify the reactivity of the SC45 which remains in any case quite low, comparable with that of undoped glass-ceramic [48].

4. Conclusions

Copper ions have been introduced, with different concentrations, in a bioactive and ferrimagnetic devitrified glass by the ion-exchange technique in molten salts, aiming to develop a magnetic, bioactive and antibacterial material for oncologic bone substitutions. Compositional

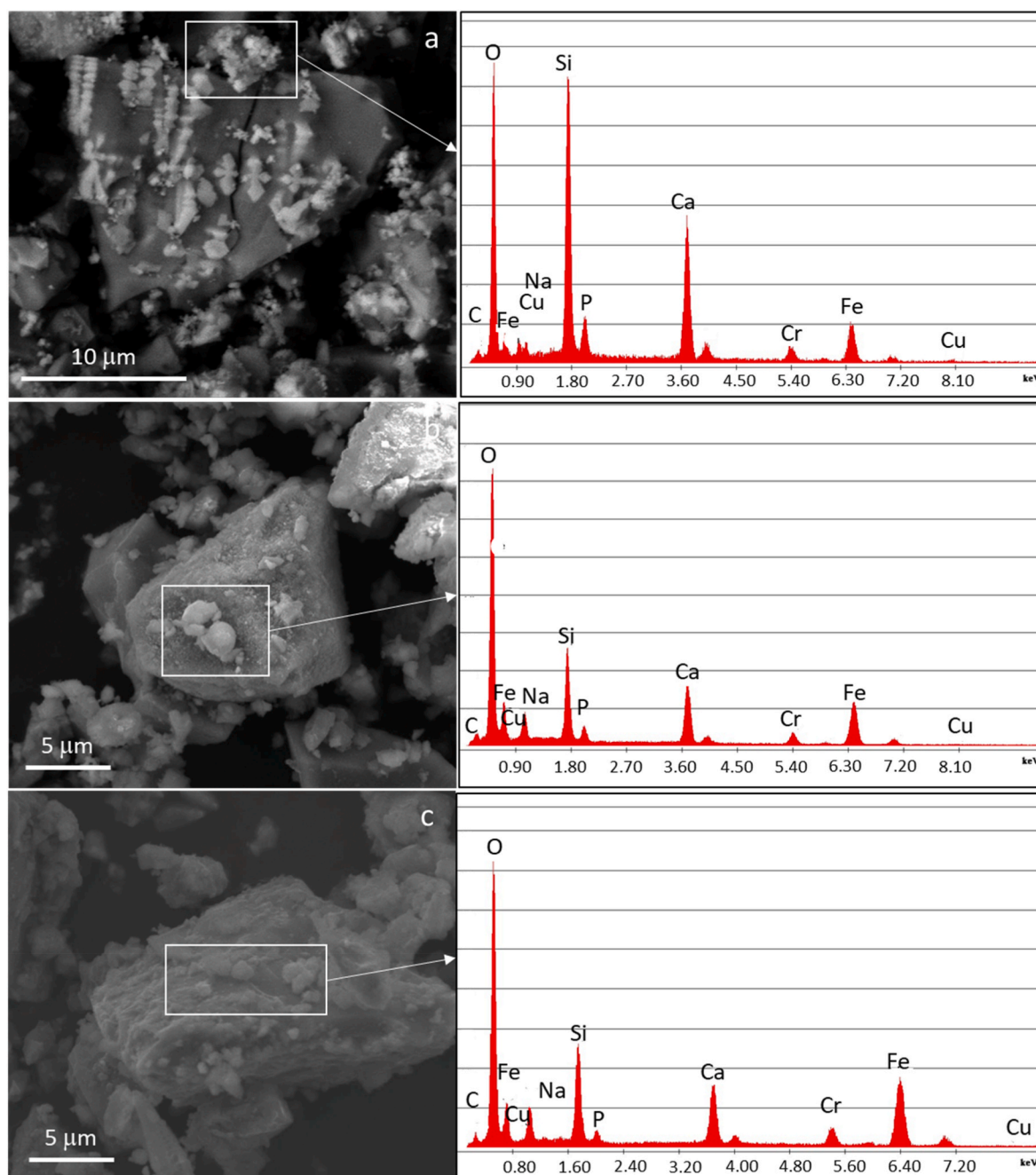


Fig. 7. SEM morphology and local EDS analysis of a) SC45 Cu 20 b) SC45 Cu 200 and c) SC45 Cu 2000 particles after 3 weeks in SBF.

and morphological analyses, supported by XRD, showed that the ion-exchange of copper involved both sodium and calcium ions and the precipitation of few amounts of copper oxide aggregates occurred, without affecting the SC45 nature of the starting material. The ion-exchange process allowed the copper introduction mostly in ionic form in the bioactive and ferrimagnetic composition, maintaining its ability to reach the temperature useful for hyperthermia under exposition to an alternating magnetic field. Samples with the highest copper amount revealed an inhibition halo correlated to a bacteriostatic effect, due to the release of copper ions, and the bioactivity test confirmed that the copper doping did not modify the reactivity of the pristine SC45.

Therefore, the obtained material, combining ferrimagnetic, bioactive and bacteriostatic properties, is promising for the treatment of bone tumor by hyperthermia and its complications (i.e. infection development). Future research will assess the material biocompatibility and its

properties in a relevant biological environment in view of the final application.

Funding

This research did not receive any specific grant from funding agencies in the public, commercial, or not-for-profit sectors.

Declaration of competing interest

The authors declare that they have no known competing financial interests or personal relationships that could have appeared to influence the work reported in this paper.

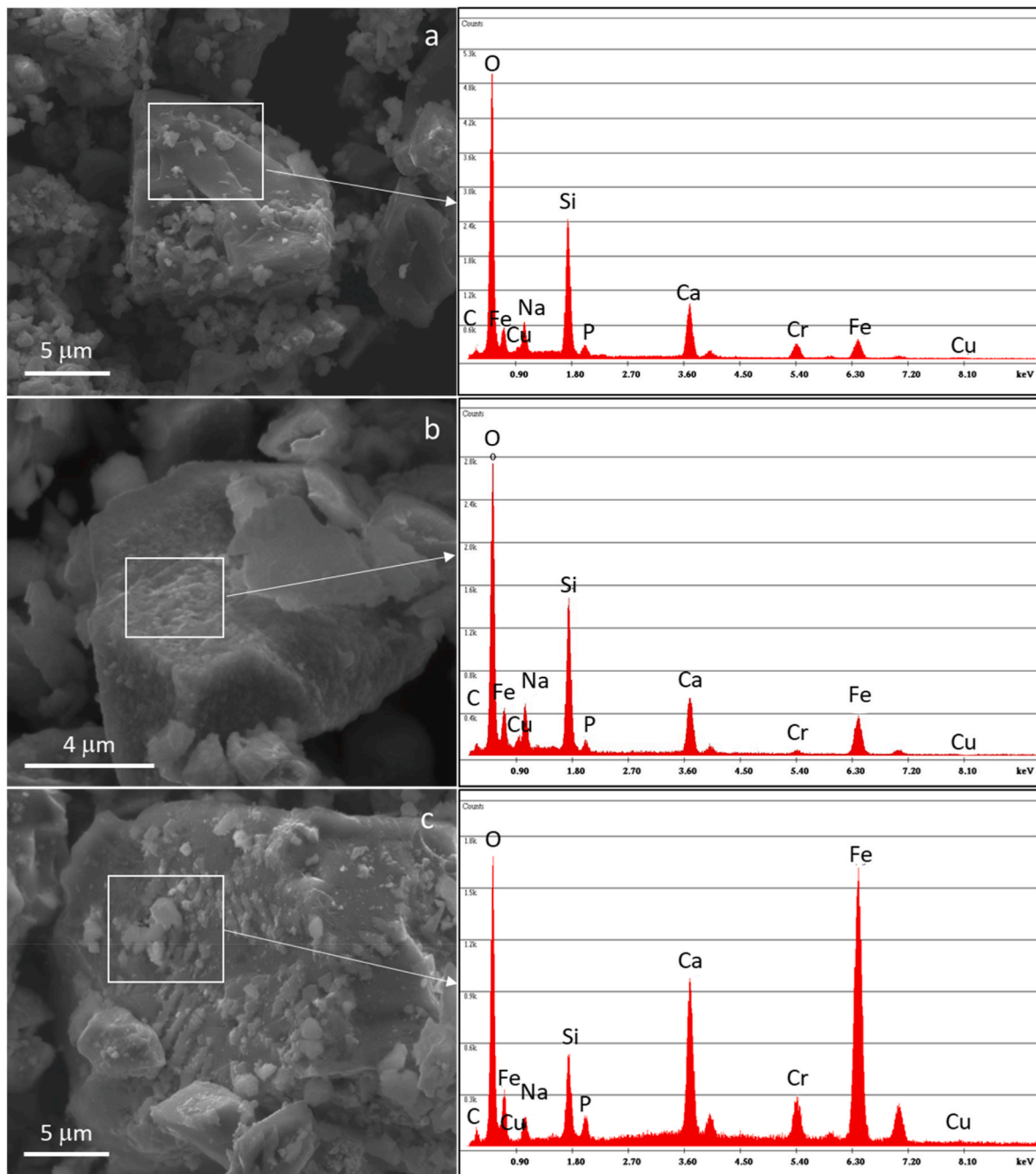


Fig. 8. SEM morphology and local EDS analysis of a) SC45_Cu 20 b) SC45_Cu 200 and c) SC45_Cu 2000 particles after 4 weeks in SBF.

References

- [1] W. Cao, L.L. Hench, Bioactive materials, *Ceram. Int.* 22 (1996) 493–507, [https://doi.org/10.1016/0272-8842\(95\)00126-3](https://doi.org/10.1016/0272-8842(95)00126-3).
- [2] L.L. Hench, *Bioceramics*, *J. Am. Ceram. Soc.* 81 (1998) 1705–1728.
- [3] R.R. Fernandes, A. Gaddam, A. Rebelo, D. Brazete, G.E. Stan, J.M.F. Ferreira, Bioactive glasses and glass-ceramics for healthcare applications in bone regeneration and tissue engineering, *Materials* 11 (12) (2018) 2530, <https://doi.org/10.3390/ma11122530>.
- [4] L.L. Hench, J.R. Jones, Bioactive Glasses, Frontiers and challenges, *Front. Bioeng. Biotechnol.* 3 (2015) 194, <https://doi.org/10.3389/fbioe.2015.00194>.
- [5] A. Hoppe, N.S. Güldal, A.R. Boccaccini, A review of the biological response to ionic dissolution products from bioactive glasses and glass-ceramics, *Biomaterials* 32 (11) (2011) 2757–2774, <https://doi.org/10.1016/j.biomaterials.2011.01.004>.
- [6] U. Pantulap, M. Arango-Ospina, A.R. Boccaccini, Bioactive glasses incorporating less-common ions to improve biological and physical properties, *J. Mater. Sci. Mater. Med.* 33 (3) (2022) 1–41. <https://link.springer.com/article/10.1007/s10856-021-06626-3>.
- [7] M. Miola, Y. Pakzad, S. Banijamali, S. Kargozar, C. Vitale-Brovarone, A. Yazdanpanah, O. Bretcanu, A. Ramedani, E. Vernè, M. Mozafari, Glass-ceramics for cancer treatment: so close, or yet so far? *Acta Biomater.* 83 (2019) 55–70, <https://doi.org/10.1016/j.actbio.2018.11.013>.
- [8] S.S. Danewalia, K. Singh, Bioactive glasses and glass-ceramics for hyperthermia treatment of cancer: state-of-art, challenges, and future perspectives, *Mater Today Bio* 24 (2021) 100100, <https://doi.org/10.1016/j.mtbio.2021.100100>.
- [9] <https://www.cancer.org/cancer/bone-cancer/about/key-statistics.html#:~:text=The%20American%20Cancer%20Society's%20Estimates,About%202%2C100%20Deaths%20visited%2005/05/2023,visited%2005/05/2023>.
- [10] <https://www.esho.info/professionals/hyperthermia/>, visited 05/05/2023.
- [11] N.R. Datta, S. Gómez Ordóñez, U.S. Gaipal, M.M. Paulides, H. Crezee, J. Gellermann, D. Marder, E. Puric, S. Bodis, Local hyperthermia combined with radiotherapy and/or chemotherapy: recent advances and promises for the future, *Cancer Treat Rev.* 41 (9) (2015) 742–753, <https://doi.org/10.1016/j.ctrv.2015.05.009>.
- [12] K. Mortezaee, A. Narmani, M. Salehi, H. Bagheri, B. Farhood, H. Haghi-Aminjan, M. Najafi, Synergic effects of nanoparticles-mediated hyperthermia in radiotherapy/chemotherapy of cancer, *Life Sci.* 269 (2021) 119020, <https://doi.org/10.1016/j.lfs.2021.119020>.

- [13] X. Liu, Y. Zhang, Y. Wang, W. Zhu, G. Li, X. Ma, Y. Zhang, S. Chen, S. Tiwari, K. Shi, S. Zhang, H.M. Fan, Y.X. Zhao, X.J. Liang, Comprehensive understanding of magnetic hyperthermia for improving antitumor therapeutic efficacy, *Theranostics* 10 (8) (2020) 3793–3815, <https://doi.org/10.7150/thno.40805>.
- [14] M. Peiravi, H. Eslami, M. Ansari, H. Zare-Zardini, Magnetic hyperthermia: potentials and limitations, *J. Indian Chem. Soc.* 99 (1) (2022) 100269, <https://doi.org/10.1016/j.jics.2021.100269>.
- [15] I.M. Obaidat, V. Narayanaswamy, S. Alaabed, S. Sambasivam, Chandu V. V. Muralee Gopi, Principles of magnetic hyperthermia: a focus on using multifunctional hybrid magnetic nanoparticles, *Magnetochemistry* (5) (2019) 67, <https://doi.org/10.3390/magnetochemistry5040067>.
- [16] A.A. Luderer, N.F. Borrelli, J.N. Panzarino, G.R. Mansfield, D.M. Hess, J.L. Brown, Glass-ceramic-mediated, magnetic-field-induced localized hyperthermia: response of a murine mammary carcinoma, *Radiat. Res.* 94 (1) (1983) 190–198.
- [17] Y. Ebisawa, T. Kokubo, K. Ohura, T. Yamamuro, Bioactivity of Fe₂O₃-containing CaO-SiO₂ glasses: in vitro evaluation, *J. Mater. Sci. Mater. Med.* 4 (1992) 225–232.
- [18] K. Masakazu, T. Hiroshi, K. Tadashi, Preparation of magnetite-containing Glass–Ceramics in Controlled atmosphere for cancer in controlled hyperthermia, *J. Ceram. Soc. Japan* 109 (2001) 39–44.
- [19] R. Kumar, G.P. Kothiyal, A. Srinivasan, Magnetic and structural properties of CaO - SiO₂ - P₂O₅ - Na₂O - Fe₂O₃ glass ceramics, *J. Magn. Mater.* 320 (2008) 1352–1356.
- [20] O. Bretcanu, S. Spriano, E. Verné, M. Coisson, P. Tiberto, P. Allia, The influence of crystallised Fe₃O₄ on the magnetic properties of coprecipitation-derived ferrimagnetic glass–ceramics, *Acta Biomater.* 1 (2005) 421–429.
- [21] O. Bretcanu, S. Spriano, C. Brovarone Vitale, E. Verne', Synthesis and characterization of coprecipitation-derived ferrimagnetic glass-ceramic, *J. Mater. Sci.* 41 (2006) 1029–1037.
- [22] O. Bretcanu, E. Verné, M. Coisson, P. Tiberto, P. Allia, Magnetic properties of the ferrimagnetic glass-ceramics for hyperthermia, *J. Magn. Magn Mater.* 305 (2006) 529–533.
- [23] O. Bretcanu, E. Verne, M. Coisson, P. Tiberto, P. Allia, Temperature effect on the magnetic properties of the coprecipitation derived ferrimagnetic glass-ceramics, *J. Magn. Magn Mater.* 300 (2) (2006) 412–417.
- [24] O. Bretcanu, M. Miola, C.L. Bianchi, I. Marangi, R. Carbone, I. Corazzari, M. Cannas, E. Verné in vitro biocompatibility of a ferrimagnetic glass-ceramic for hyperthermia application, *Mater. Sci. Eng. C* 73 (2017) 778–787, <https://doi.org/10.1016/j.msec.2016.12.105>.
- [25] A. Saqlain, M.U. Shah, S. Hashmi, A. Alam, A. Shamim, Magnetic and bioactivity evaluation of ferrimagnetic ZnFe₂O₄ containing glass ceramics for the hyperthermia treatment of cancer, *J. Magn. Magn Mater.* 322 (3) (2010) 75–81.
- [26] M. Baikousi, S. Agathopoulos, I. Panagiotopoulos, A.D. Georgoulis, M. Louloudi, M. A. Karakassides, Synthesis and characterization of sol–gel derived bioactive CaO–SiO₂–P₂O₅ glasses containing magnetic nanoparticles, *J. Sol. Gel Sci. Technol.* 47 (2008) 95–101.
- [27] F. Baino, E. Fiume, M. Miola, F. Leone, B. Onida, F. Laviano, R. Gerbaldo, E. Verné, Fe-doped sol-gel glasses and glass-ceramics for magnetic hyperthermia, *Materials* 11 (2018) 173, <https://doi.org/10.3390/ma11010173>.
- [28] F. Baino, E. Fiume, M. Miola, F. Leone, B. Onida, E. Verné, Fe-doped bioactive glass-derived scaffolds produced by sol-gel foaming, *Mater. Lett.* 235 (2019) 207–211.
- [29] R. Borges, L.M. Ferreira, C. Rettori, I.M. Lourenço, A.B. Seabra, F.A. Muller, E. Prado Ferraz, M.M. Marques, M. Miola, F. Baino, J.B. Mamani, L.F. Gamarra, J. Marchi, Superparamagnetic and highly bioactive SPIONS/bioactive glass nanocomposite and its potential application in magnetic hyperthermia, *Mater. Sci. Eng. C* 135 (2022) 112655, <https://doi.org/10.1016/j.msec.2022.112655>.
- [30] N. Shankhwar, A. Srinivasan, Evaluation of sol-gel based magnetic 45S5 bioglass and bioglass–ceramics containing iron oxide, *Mater. Sci. Eng., C* 62 (2016) 190–196.
- [31] E. Verné, M. Miola, S. Ferraris, C.L. Bianchi, A. Naldoni, G. Maina, O. Bretcanu, Surface activation of a ferrimagnetic glass–ceramic for antineoplastic drugs grafting, *Adv. Eng. Mater.* 12 (7) (2010) B309–B319, <https://doi.org/10.1002/adem.200980082>.
- [32] M. Bruno, M. Miola, O. Bretcanu, C. Vitale-Brovarone, R. Gerbaldo, F. Laviano, E. Verne, Composite bone cements loaded with a bioactive and ferrimagnetic glass-ceramic. Part I: morphological, mechanical and calorimetric characterization, *J. Biomater. Appl.* 29 (2) (2014) 254–267, <https://doi.org/10.1177/0885328214521847>.
- [33] E. Verné, M. Bruno, M. Miola, G. Maina, C. Bianco, A. Cochis, L. Rimondini, Composite bone cements loaded with a bioactive and ferrimagnetic glass ceramic: leaching, bioactivity and cytocompatibility, *Mater. Sci. Eng. C* 53 (2015) 95–103, <https://doi.org/10.1016/j.msec.2015.03.039>.
- [34] M. Miola, F. Laviano, R. Gerbaldo, M. Bruno, A. Lombardi, A. Cochis, L. Rimondini, E. Verné, Composite bone cements for hyperthermia: modeling and characterization of magnetic, calorimetric and in vitro heating properties, *Ceram. Int.* 43 (2017) 4831–4840, <https://doi.org/10.1016/j.ceramint.2016.12.049>.
- [35] M. Miola, R. Gerbaldo, F. Laviano, M. Bruno, E. Verné, Multifunctional ferrimagnetic glass–ceramic for the treatment of bone tumor and associated complications, *J. Mater. Sci.* 52 (2017) 9192–9201, <https://doi.org/10.1007/s10853-017-1078-6>.
- [36] M. Miola, M. Bruno, R. Gerbaldo, F. Laviano, E. Verné, Melt-derived copper-doped ferrimagnetic glass-ceramic for tumor treatment, *Ceram. Int.* 47 (2021) 31749–31755, <https://doi.org/10.1016/j.ceramint.2021.08.056>.
- [37] R. Koohkan, T. Hooshmand, D. Mohebbi-Kalhari, M. Tahriri, M. Taha Marefati, Synthesis, characterization, and in vitro biological evaluation of copper-containing magnetic bioactive glasses for hyperthermia in bone defect treatment, *ACS Biomater. Sci. Eng.* 4 (5) (2018) 1797–1811, <https://doi.org/10.1021/acsbomaterials.7b01030>. Epub 2018 Mar 20.
- [38] F.N.S. Raja, T. Worthington, R.A. Martin, The antimicrobial efficacy of copper, cobalt, zinc and silver nanoparticles: alone and in combination, *Biomed. Mater.* 18 (2023) 045003, <https://doi.org/10.1088/1748-605X/acd03f>.
- [39] I. Codiță, D.M. Caplan, E.C. Drăgulescu, B.E. Lixandru, I.L. Coldea, C. C. Dragomirescu, C. Surdu-Bob, M. Bădulescu, Antimicrobial activity of copper and silver nanofilms on nosocomial bacterial species, *Roum. Arch. Microbiol. Immunol.* 69 (4) (2010) 204–212.
- [40] Performance Standards for Antimicrobial Disk Susceptibility Tests, Approved Standard M2-A9, ninth ed., NCCLS, Villanova, PA, USA, 2003.
- [41] M. Miola, E. Verné, Bioactive and antibacterial glass powders doped with copper by ion-exchange in aqueous solutions, *Materials* 9 (2016) 405–421, <https://doi.org/10.3390/ma9060405>.
- [42] S. Karlsson, S. Reibsteif, Surface ruby colouring of float glass by sodium-copper ion exchange, *Glas, Technol. Eur. J. Glas. Sci. Technol. A* 54 (2013) 100–107.
- [43] M. Lallukka, M. Miola, Z. Najmi, A. Cochis, S. Spriano, L. Rimondini, E. Verné, Cu-doped bioactive glass with enhanced in vitro bioactivity and antibacterial properties, *Ceramics International*, available online 22 November, <https://doi.org/10.1016/j.ceramint.2023.11.253>, 2023.
- [44] M. Vincent, R.E. Duval, P. Hartemann, M. Engels-Deutsch, Contact killing and antimicrobial properties of copper, *J. Appl. Microbiol.* 124 (5) (2018) 1–15, <https://doi.org/10.1111/jam.13681>.
- [45] D.A. Montero, C. Arellano, M. Pardo, R. Vera, R. Gálvez, M. Cifuentes, M. A. Berasain, M. Gómez, C. Ramírez, R.M. Vidal, Antimicrobial properties of a novel copper-based composite coating with potential for use in healthcare facilities, *Antimicrob. Resist. Infect. Control* 8 (2019) 3, <https://doi.org/10.1186/s13756-018-0456-4>.
- [46] Marta Miola, Elisa Bertone, Enrica Verné, In situ chemical and physical reduction of copper on bioactive glass surface, *Appl. Surf. Sci.* 495 (2019) 143559, <https://doi.org/10.1016/j.apsusc.2019.143559>. ISSN 0169-4332.
- [47] M. Hans, A. Erbe, S. Mathews, Y. Chen, M. Solioz, F. Mücklich, Role of copper oxides in contact killing of Bacteria, *Langmuir* 29 (2013) 16160–16166, <https://doi.org/10.1021/la404091z>.
- [48] E. Verné, M. Miola, S. Ferraris, C.L. Bianchi, A. Naldoni, G. Maina, O. Bretcanu, Surface activation of a ferrimagnetic glass-ceramic for antineoplastic drugs, *Advanced Biomaterials* 12 (2010) B309–B319, <https://doi.org/10.1002/adem.200980082>.